Chapter 6

Theory of ENSO Sensitivity to Climate

All perception of truth is the detection of an analogy.

Thoreau, *Journal*, 1851

In this chapter we examine the role of the background state in the dynamics of ENSO, by examining the processes that drive sea surface temperature changes in the equatorial Pacific. We first review the primary modes that contribute to interannual oscillations, and examine previous model results regarding the sensitivity of ENSO to the climatology. We then investigate the influence of nonlinearity and the climatology on these modes and propose a way of distinguishing between them based on the relative phasing of terms in the SST tendency equation. Phasor diagrams prove useful for clarifying the individual roles of the tendency terms and their sensitivities to climate change.

6.1 Literature review

6.1.1 Prototype modes

Comprehensive reviews of ENSO theory are given by Neelin et al. (1998) and Philander (1999). In this section we shall focus only on the aspects most relevant to understanding the ENSO sensitivity to the tropical climatology. Two basic types of coupled ocean-atmosphere modes appear relevant to the observed ENSO: a "delayed-oscillator" or "recharge" mode (Fig. 6.1) which depends on slow oceanic adjustment to remote wind forcing (Wyrtki, 1985; Schopf and Suarez, 1988; Suarez and Schopf, 1988; Battisti and Hirst, 1989; Schneider et al., 1995; Jin, 1996; Li, 1997; Jin, 1997), and "SST" modes (Fig. 6.2) that depend more on local wind forcing, anomalous zonal currents, and anomalous upwelling (Zebiak, 1985; Hirst, 1986; Neelin, 1991; Hao et al., 1993; Jin and Neelin, 1993a,b; Dijkstra and Neelin, 1999). ENSO in the real world appears to be a hybrid mode, with ocean adjustment setting the time scale and the SST mode setting the spatial structure and propagation

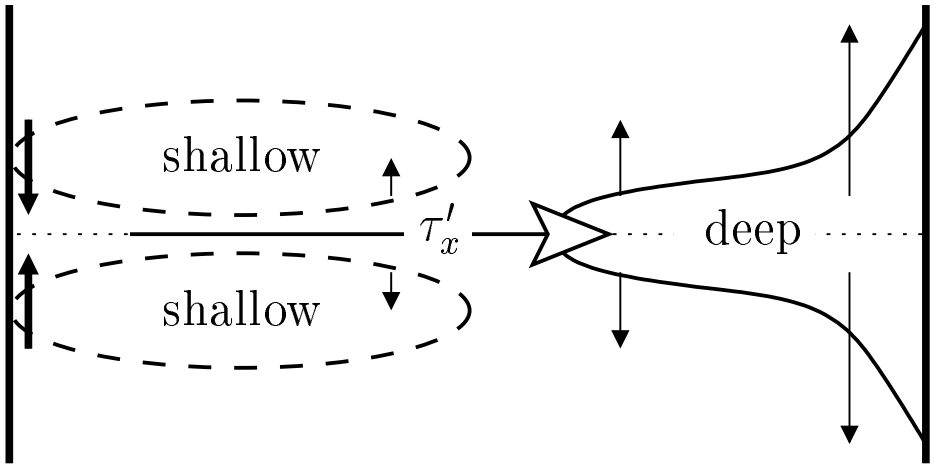

Figure 6.1: View of the recharge/delayed oscillator mode from above. An equatorially-confined westerly stress anomaly induces a rapid deepening of the thermocline in the equatorial eastern Pacific, which warms the surface there via mean upwelling and enhances the westerly stress anomaly. Meanwhile, strong cyclonic stress curl off-equator induces a broad shoaling of the thermocline in the western Pacific and slowly discharges warm water from the equatorial zone. Narrow western boundary currents return some warm water to the equator but not enough to compensate for the discharge in the interior. As the equatorial thermocline shoals, the warm event decays as the remaining wind forcing continues discharging water from the equator. The system is then carried into a cold event by an anomalously shallow equatorial thermocline and associated westward current anomalies, and the cycle repeats with opposite sign.

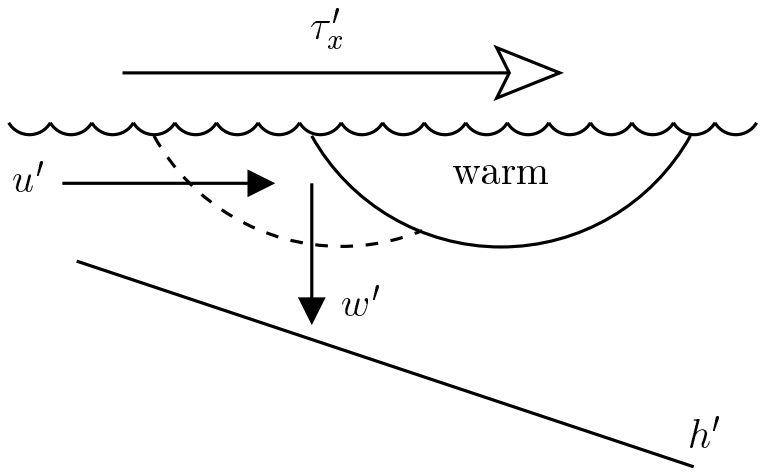

Figure 6.2: Structure of the SST mode, represented as a vertical section through the oceanic active layer and lower troposphere at the equator. A warm anomaly induces anomalous westerly wind stress to the west, which induces downwelling anomalies local to the stress and westerly current anomalies slightly west of the stress. The anomalous currents thus favor *westward* propagation by acting on the mean upward and westward thermal gradients to induce warming to the west of the warm anomaly. In the fast-wave limit, the thermocline is anomalously deep to the east of the stress anomaly, which favors *eastward* propagation of the SST anomaly if the mean upwelling is strong enough.

of SST anomalies (Jin and Neelin, 1993a). If the modal period is long enough (a few years), as appears to be the case for the observed ENSO, individual Kelvin and Rossby wavefronts may not be apparent; hence the relevance of a "fast-wave limit" for the SST mode in which the subsurface ocean is assumed to adjust instantaneously to the wind stress (Neelin, 1991). Variability at shorter periods (a year or less), on the other hand, can evolve as a coupled Rossby mode that depends primarily on zonal advection at the equator and resonant interactions with the eastern and western boundaries (Hirst, 1986; Mantua and Battisti, 1995); such modes have been found to play a role in some models (e.g. that of Zebiak and Cane, 1987).

The zonal propagation of SST anomalies in the fast-wave limit is set by a competition between "thermocline feedbacks" and "local" or "advective" feedbacks (Hirst, 1985, 1986, 1988; Hao et al., 1993; Jin and Neelin, 1993a; An and Jin, 2000, 2001). Thermocline feedbacks are associated with the equatorial thermocline slope, which responds fairly rapidly to changes in zonal wind stress; a westerly stress anomaly induces a deepening of the thermocline in the east, which warms the surface in the east through mean upwelling and drags the stress anomaly eastward. The local advective feedbacks are associated with the anomalous zonal currents and upwelling, which respond locally to stress anomalies that are generally shifted west of the SST anomalies; a warm SST anomaly induces westerlies to the west, which induce local downwelling and eastward currents that drag the SST anomaly westward. Thus thermocline and local advective feedbacks tend to favor eastward and westward propagation, respectively. If both feedbacks are present, the propagation

can be slowed or halted; in the latter case, a standing SST oscillation may arise if oceanic adjustment is delayed.

The stability and period of the delayed/recharge oscillator likewise results from a competition of feedbacks (Battisti and Hirst, 1989; Jin, 1997; An and Jin, 2001). The first is local growth in the equatorial eastern Pacific, which is accomplished by a basinwide positive feedback: during El Niño, the trade winds slacken and deepen the thermocline in the east, which inhibits cooling of the surface in the east, weakens the zonal SST gradient, and thereby further weakens the trades. The second process is a delayed negative feedback that results from slow adjustment of the thermocline. In response to meridionally-confined wind anomalies such as occur during ENSO, geostrophic divergence in the interior and western boundary currents discharge (during El Niño) or recharge (during La Niña) warm surface waters at the equator, which raises or lowers the thermocline in opposition to the eastern Pacific anomaly generated by the zonal slope of the thermocline. Eventually, this slow adjustment affects the surface waters sufficiently to bring about a reversal of the event. Zonal currents, which are linked geostrophically to the zonal-mean thermocline depth at the equator, also contribute to the decay by advecting cold water westward (following an El Niño) or warm water eastward (following La Niña). The combination of rapid adjustment of the equatorial thermocline slope, and delayed adjustment of the equatorial zonal-mean thermocline induced by off-equatorial ocean memory, are thus essential for this mode. The period and growth rate of this delayed/recharge oscillator are surprisingly complex functions of the adjustment time, the strength of the delayed feedbacks, and the strength of local growth processes in the eastern equatorial Pacific (Battisti and Hirst, 1989).

These "prototype modes" can be hard to characterize simply by looking at SST; their similar spatial structures can belie their internal mechanisms and thus their sensitivities to externally-imposed changes. The best way to distinguish them is to examine the balances and relative phasings of the processes which affect SST. We shall develop a framework for this in Sections 6.2 and 6.3.

6.1.2 Influence of the background state

On equatorial waves

From the shallow-water equations (4.1)–(4.3) it is evident that the depth of the thermocline affects the speed and amplitude of equatorial waves. Using an intermediate model, Zebiak and Cane (1987) found that a shoaling of the zonal-mean thermocline, by amplifying the thermocline-slope response to wind stress and delaying the adjustment of the zonal-mean thermocline to changes in wind stress, tended to increase the amplitude and period of ENSO; Dewitte (2000) found similar results. Other authors have expanded on how the structure of the climatology can influence the amplitude, propagation, and dispersion of Kelvin and Rossby waves in a multilevel ocean (Busalacchi and Cane, 1988; Yang, 1991; Yang and Yu, 1992; Yang and O'Brien, 1993).

The background state can also affect the propagation of equatorial waves in the atmosphere. Wang and Xie (1996) found that increased mean vertical westerly wind shear tended to weaken Rossby waves in the lower troposphere, with little impact on Kelvin

waves. Since it is the Rossby component that conveys the westerly stress response westward from regions of anomalous heating, it is conceivable that a long-term change in the strength of the Walker Cell could affect the structure of the wind stress response to SST anomalies. The mean vertical wind shear can also affect the surface stress profile of intraseasonal convective disturbances like the MJO, which appear to be important for modifying ENSO evolution. Takayabu et al. (1999), for example, argued that background westerly shear contributed to the rapid demise of the 1997–98 El Niño: westerly shear altered an MJO disturbance so that it produced predominantly easterly stress anomalies, which in May 1998 reinitiated upwelling on an unusually strong subsurface temperature gradient in the eastern Pacific.

In conceptual models

Results from simple conceptual models provide some insight into the climate sensitivities of ENSO. Battisti and Hirst (1989) analyzed a simple delayed-oscillator model, and found that a strengthening of local growth mechanisms in the east Pacific, or an increase in the delay time for negative feedbacks, favored longer-period and faster-growing oscillations. A strengthening of the delayed feedbacks, on the other hand, favored stronger and shorter-period oscillations. Pure growth and no oscillations obtained if the local growth mechanisms were too strong relative to the delayed feedbacks.

Jin (1996) explored the sensitivity of ENSO to the tropical climatology using a conceptual model of the recharge oscillator. He found that ENSO did not occur if the climatological cold tongue/trade winds were too weak, since a lack of equatorial mean upwelling resulted in SST being too insensitive to thermocline motions in the east. ENSO also did not occur if the cold tongue was too strong, since in this case waters could get no colder in the east and SST again became insensitive to thermocline motions.

In intermediate models

Several studies in intermediate-complexity models have also investigated the sensitivity of ENSO to the climatological background state. Wakata and Sarachik (1991, 1992), building on the work of Hirst (1988), explored the sensitivities of equatorial coupled modes in a bounded basin. They found that both increased air-sea coupling and increased mean upwelling tended to favor oscillations with stronger growth rates and longer periods. Growth rates also tended to increase with the zonal tilt of the thermocline, the strength of the east-west SST contrast, and the meridional width of the equatorial upwelling. The upwelling width also strongly affected the period and propagation tendency of the unstable modes: narrow upwelling inhibited the influence of the thermocline on the surface, favoring zonal advective mechanisms and a westward-propagating mode, while wide upwelling favored thermocline mechanisms and an eastward-propagating mode.

Dijkstra and Neelin (1999) examined the ENSO sensitivity to trade wind strength using the simple model of Jin and Neelin (1993a), with coupled climatologies simulated as in Dijkstra and Neelin (1995). They found only a small region of model parameter space that supported both a realistic climatology and a realistic ENSO, and both were very sensitive to the external component of the trade winds. With increasing air-sea coupling,

the climatology became more La Niña-like, the subsurface temperature saturated in the eastern Pacific, SST in the east became less sensitive to wave dynamics, local growth mechanisms (such as $-u'\partial_x\overline{T}$ and $-w'\partial_z\overline{T}$) dominated the delayed feedbacks, and thus ENSO did not occur. At moderate coupling, oscillations were possible, but only when the tradewind forcing was strong enough that delayed thermocline feedbacks were sufficient to transition the system between warm and cold events. The ENSO frequency was found to increase with increasing trade wind strength. As in Jin (1996), the oscillations were most robust at intermediate wind strength, where coupled feedbacks were strong enough to produce ENSO growth, but not so strong as to produce saturation of the climatological subsurface temperature in the eastern Pacific.

Attempting to explain observed decadal changes in ENSO, Wang and An (2002) explored the ENSO sensitivity to a zonal shift in the climatological tradewinds by prescribing two different background states in the Zebiak and Cane (1987) model. These climatologies were interpolated between the standard model climatology and observed decadal averages from before and after the 1976–77 climate shift, corresponding to an eastward shift in the trade winds. The former case gave a weak ENSO with a 3-year period and westward propagation, while the latter gave a strong ENSO with a 4-year period, eastward propagation, and an eastward shift of the variability relative to the former case. The authors argued for the primacy of the zonal shifts in wind convergence and mean upwelling between the two climatologies, which caused corresponding shifts in the sensitivity of the winds to SST and the sensitivity of the zonal SST gradient to thermocline motions. These changes, by shifting anomalous variability eastward, also lengthened the ENSO period by increasing the time required for negative feedbacks (associated with Rossby waves) to reflect from the western boundary. The increased delay, in turn, enhanced the amplitude of ENSO by allowing more time for growth due to air-sea feedbacks in the eastern basin. The shift in propagation from westward to eastward was identified with a shift in mechanism from $-u'\partial_x\overline{T}$ to $-\overline{w}\partial_z T'$, due to a reduction in the climatological zonal SST contrast in the central Pacific and an increase in mean upwelling the eastern Pacific. An and Jin (2000) and Wang and An (2001) likewise investigated the consequences for ENSO of the 1976 climate shift (see Section 1.1.6).

Other clues are provided by studies that investigated the role of seasonal variations in the background state on the behavior of ENSO. Zebiak and Cane (1987) and Battisti and Hirst (1989) found that climate anomalies tend to be seeded in boreal spring, when the ITCZ is close to the equator, and then grow in boreal summer, as the equatorial upwelling and zonal SST gradient strengthen. Wang and Fang (1996), using a simpler conceptual model, found peak instability in boreal spring, arguing that it was due to the strong vertical temperature gradient (which enhanced positive feedbacks) and weakened upwelling (which reduced negative feedbacks) at that time of year. Wang and Fang (2000), using a more complete intermediate model, examined runs with perpetual-April and perpetual-October radiative forcing. The April case, which produced an El Niño-like background state with weak upwelling and weak vertical temperature gradients, supported longer-period interannual oscillations than the October case which produced a more La Niña-like climatology.

Several studies with intermediate models have mapped the properties of the prototype

modes as a function of changes in key *dynamical* parameters, such as the air-sea coupling strength, the oceanic adjustment time, the strength of currents in the surface layer, and the strength of damping by surface fluxes (Neelin, 1991; Hao et al., 1993; Jin and Neelin, 1993a,b; Neelin and Jin, 1993). To connect these results with observable *climate* parameters, Fedorov and Philander (2000, 2001) prepared complementary maps of the linear stability properties of these modes as a function of the strength of the mean trade winds, the zonal-mean depth of the thermocline, and the sharpness of the thermocline in the vertical. Two important results from these studies are that the linear behavior of ENSO can be very sensitive to parameter and climate changes, and that the sensitivity itself can depend critically on where one stands in parameter space. Perigaud et al. (2000b) and Fedorov (2002) extended some of these results to the time-dependent regime, showing how the response of the coupled ocean-atmosphere system to westerly wind bursts can be sensitive to the depth of the equatorial thermocline.

In coupled GCMs

A number of studies with coupled GCMs have investigated the influence of the background state on interannual variability. Moore (1995) examined the influence of climatological flux adjustments in a coupled GCM. The unadjusted model exhibited a fairly uniform cold bias with weak trades and a thermocline that was too flat, and interannual variability resembling a westward-propagating SST mode. With flux adjustments of surface heat and freshwater only, the model produced an El Niño-like warming of the mean state, and eastward-propagating SST anomalies. Additional flux adjustment of the wind stress produced stronger mean trades and upwelling, and a westward-propagating SST mode amplified by an enhanced convective response to SST anomalies. Increasing the air-sea coupling led to the emergence of delayed-oscillator modes in both the unadjusted and fully flux-adjusted versions of the model.

Li and Hogan (1999) also examined the influence of flux adjustments in a coupled GCM. Their unadjusted model had a climatological cold tongue that was detached from the eastern boundary, and supported only a weak westward-propagating SST mode. With flux adjustments, the cold tongue attached to the eastern boundary, the east-west SST contrast increased, and the simulated ENSO became stronger.

Gordon et al. (2000) explored the influence of low clouds on the climatology and variability of a coupled GCM, which in its control state with simulated clouds showed an El Niño-like warm bias. Specifying only 80% of the observed marine stratocumulus clouds enhanced the cold tongue and produced stronger ENSO variability. Specifying the full observed stratocumulus produced an even stronger cold tongue, with *weaker* ENSO variability than in the control. The ENSO spectra were similar among these cases, but that a 20% change in climatological stratus could have such a large effect on the ENSO amplitude was surprising.

Codron et al. (2001) found that changing a few parameterizations in their coupled GCM produced an El Niño-like warming of the mean state, and an ENSO that was stronger, had a longer period and produced SST anomalies that were stationary instead of westward-propagating. The authors argued that these ENSO changes in the updated model were

due to a strengthening of the wind stress response to SST anomalies, a reduction in the off-equatorial wind stress curl (which reduced the effects of negative feedbacks on zonal average thermocline depth at the equator), and the better confinement of the stress anomalies to the western/central Pacific.

6.1.3 Summary

Several important points have emerged from this review. First, the SST mode and the delayed/recharge oscillator are useful prototypes for describing the time scale, growth rate, spatial structure, and propagation characteristics of ENSO in observations and models. Second, the behavior of these modes, and the merger between them, is controlled by the structure of the background state. The climatology affects the propagation of equatorial waves, the nature of the air/sea coupling, and the strength of the direct and delayed feedbacks that are essential for oscillations and growth. Studies with intermediate models and coupled GCMs have demonstrated the importance to ENSO behavior of the air-sea coupling strength, the structure of the wind stress response to SST anomalies, and the relative balance of thermocline feedbacks and local advective feedbacks. Key climate parameters that appear to affect ENSO in climate models are the depth of the thermocline in the eastern equatorial Pacific, the strength of the zonal SST gradient along the equator, the strength and width of the equatorial mean upwelling, and the intensity of surface wind convergence near the equator.

Although the sensitivities of ENSO are complex, it should be possible to summarize them in a clear diagram that illustrates the relative importance and phasing of the various processes that affect SST. Such a diagram should permit a clear identification of the mechanism in a given model, afford an easy comparison with other models, and also lend insight into climate sensitivities. The next two sections develop just such a diagram, which will be used to support the analyses of the intermediate model and GCM simulations in Chapter 7.

6.2 ENSO sensitivity in the intermediate model

6.2.1 Linearization of the SSTA tendency

The role of the climatology in ENSO evolution is clarified by examining small perturbations about the climatology. We will concentrate on regions of mean upwelling, namely the cold tongue, since these show the largest SST variations during ENSO. Under these conditions the nonlinearities in the SSTA tendency equation (4.28) are weak, and so a linearized version is appropriate:

$$\begin{aligned} \partial_t T'\big|_{linear} \;=\; & -(u'\partial_x + v'\partial_y + w'\partial_z)\overline{T} \\ & -(\overline{u}\partial_x + \overline{v}\partial_y + \overline{w}\partial_z)T' \\ & +(\kappa\nabla^2 - \epsilon)T' \end{aligned} \tag{6.1}$$

For the intermediate model, we may further linearize the entrainment temperature dependence on thermocline depth by assuming $T'_e \approx bh'$. It is also useful to decompose the

thermocline depth anomaly into a zonal-mean part h'_m and a zonal-perturbation part h'_p. The effect of subsurface temperature changes on SST is then given by the sum of three terms:

$$-\overline{w}\partial_z T' = \frac{\gamma\overline{w}}{H_m}\left(bh'_m + bh'_p - T'\right) \tag{6.2}$$

6.2.2 Local dispersion relation

To understand the effects of these processes on SST evolution during ENSO, we may examine the evolution of a normal mode:

$$\left(T', u', v', w'\right) = \mathrm{Re}\left[\left(\widetilde{T}', \widetilde{u}', \widetilde{v}', \widetilde{w}'\right) e^{\omega t}\right] \tag{6.3}$$

where ω is the complex frequency of the mode, and $\left(\widetilde{T}', \widetilde{u}', \widetilde{v}', \widetilde{w}'\right)$ are complex amplitudes which vary with location. Applying (6.1) to (6.3) yields the dispersion relation

$$\begin{aligned}\omega \;=\; & -\frac{\widetilde{u}'}{\widetilde{T}'}\partial_x\overline{T} - \frac{\widetilde{v}'}{\widetilde{T}'}\partial_y\overline{T} - \frac{\widetilde{w}'}{\widetilde{T}'}\partial_z\overline{T} \\ & -\overline{u}\frac{\widetilde{\partial_x T'}}{\widetilde{T}'} - \overline{v}\frac{\widetilde{\partial_y T'}}{\widetilde{T}'} - \overline{w}\frac{\widetilde{\partial_z T'}}{\widetilde{T}'} \\ & +\kappa\frac{\widetilde{\nabla^2 T'}}{\widetilde{T}'} - \epsilon\end{aligned} \tag{6.4}$$

This says that ω is controlled by the amplitudes and phases of the tendency terms *relative* to those for SSTA, since for complex numbers ψ_1 and ψ_2,

$$\frac{\psi_2}{\psi_1} = \frac{|\psi_2|}{|\psi_1|}\exp\left[i\left(\theta_{\psi_2} - \theta_{\psi_1}\right)\right] \tag{6.5}$$

where $\theta_{\psi_2} - \theta_{\psi_1}$ is the phase lead of ψ_2 ahead of ψ_1.

For the intermediate model, we may further apply the normal mode structure to the vertical advection term to yield

$$-\overline{w}\frac{\widetilde{\partial_z T'}}{\widetilde{T}'} = \frac{\gamma\overline{w}b}{H_m}\left(\frac{\widetilde{h}'_m}{\widetilde{T}'} + \frac{\widetilde{h}'_p}{\widetilde{T}'}\right) - \frac{\gamma\overline{w}}{H_m} \tag{6.6}$$

6.2.3 Local phase relationships

The dispersion relation (6.4) is illustrated in Fig. 6.3, as a sum of the dominant temperature tendency terms in the complex plane. This schematic, which is loosely based on the intermediate model control run (Fig. 4.21), gives a sort of "frequency budget" for a hypothetical growing mode. The angle of each tendency term from the positive real axis indicates its phase lead ahead of SSTA, so the effect of each term on the mode stability is clear. A stabilizing term is associated with a vector that points to the left; a destabilizing term is associated with a vector that points to the right. An upward-pointing vector (90° phase lead) corresponds to a term which has no effect on stability, but instead contributes

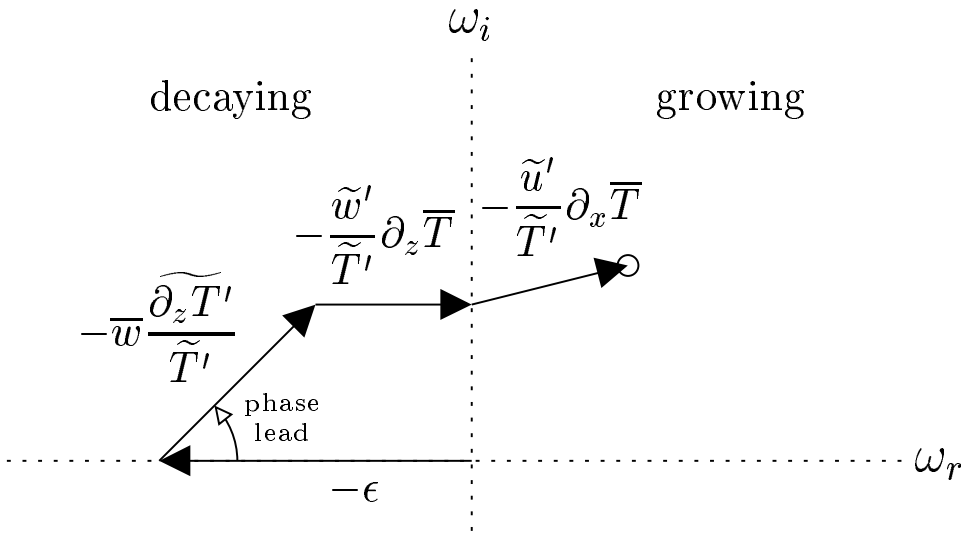

Figure 6.3: Schematic illustration of the complex frequency of SST anomalies (circle), which results from a combination of advective and surface flux tendencies (vectors). Real axis (ω_r) is the e-folding growth rate of the SSTA envelope: positive is growing, negative is decaying. Imaginary axis (ω_i) is the angular frequency in time. The counter-clockwise angle of each vector from the positive real axis indicates its phase lead ahead of SSTA.

to the oscillation itself, as an "inertia" which carries the system past equilibrium points. Conversely, a vector that points downward (90° phase lag) corresponds to an "anti-inertial" term which opposes oscillations and acts to decrease their frequency.

In the control run the surface heat flux is a pure damping term, so it is 180° out of phase with SSTA. The *linear* dependence of the heat flux on SSTA further implies there is a fundamental timescale, ϵ^{-1}, which is independent of location or amplitude. Plotted as the first term in the vector sum, the surface flux provides an invariant scale and "anchor" for the remaining terms.

For the hypothetical mode pictured in Fig. 6.3, the $-\frac{\widetilde{w}'}{\widetilde{T}'}\partial_z\overline{T}$ term associated with anomalous upwelling has a phase angle of 0°. This is because the zonal stress, which is the main driver of equatorial upwelling, is in phase with SSTA over most of the basin. The westerly stress response to warm events induces Ekman convergence and downwelling at the equator, reducing the inflow of cold water from the deep. As a result, $-\frac{\widetilde{w}'}{\widetilde{T}'}\partial_z\overline{T}$ is a pure destabilizer which opposes damping and tries to push the system away from equilibrium.

The $-\overline{w}\frac{\widetilde{\partial_z T'}}{\widetilde{T}'}$ and $-\frac{\widetilde{u}'}{\widetilde{T}'}\partial_x\overline{T}$ tendency terms are also destabilizers: anomalous westerly stress produces anomalous eastward flow and a deepening of the thermocline in the east, both of which act to warm SST in the east and enhance the westerly stress. These feedbacks are not coincident with SSTA, however, and therefore play a role in the transitions between events. Because they lead SSTA, these terms serve to increase the frequency of the oscillations by accelerating the system through the equilibrium state.

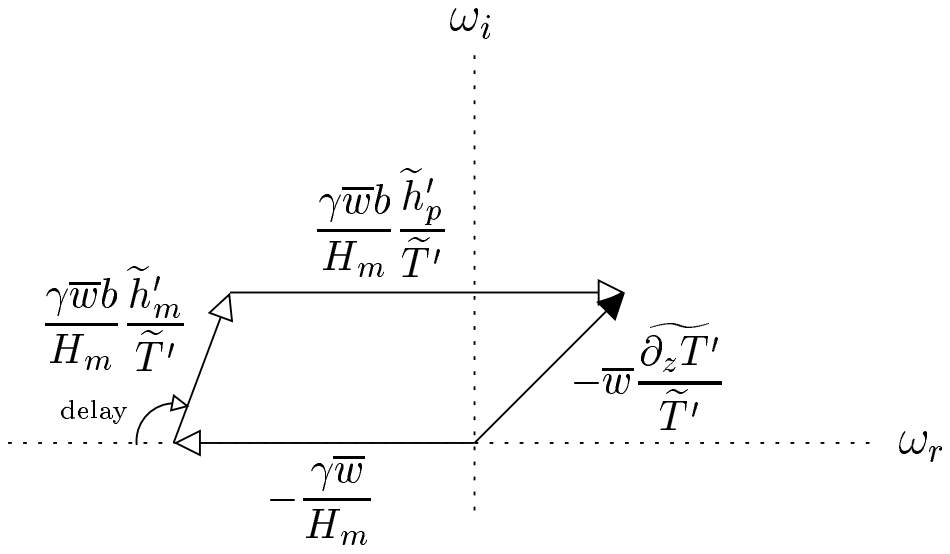

Figure 6.4: Resolution of the frequency effect of equatorial eastern Pacific subsurface temperature changes, $-\overline{w}\frac{\widetilde{\partial_z T'}}{\widetilde{T}'}$, into three components: an SSTA damping $-\frac{\gamma\overline{w}}{H_m}$, a positive feedback $\frac{\widetilde{h}'_p}{\widetilde{T}'}$ from the rapid adjustment of the thermocline slope, and a delayed negative feedback $\frac{\widetilde{h}'_m}{\widetilde{T}'}$ from the slow adjustment of the zonal-mean thermocline depth. Otherwise as in Fig. 6.3.

The complex role of these terms arises from the combined effects of direct feedbacks, associated with rapid adjustment of the equatorial thermocline slope via equatorial Kelvin waves, and delayed negative feedbacks, associated with slow adjustment of the zonal-mean thermocline depth through off-equatorial Rossby waves and boundary reflections. To illustrate for $-\overline{w}\frac{\widetilde{\partial_z T'}}{\widetilde{T}'}$, we refer to (6.6) and concentrate on regions of mean upwelling so that all parameters in that equation are positive. Fig. 6.4 illustrates this sum in the complex plane, with phasors appropriate for the eastern equatorial Pacific in both the intermediate model and observations (Jin, 1997; An and Kang, 2000).

The pure damping effect of $-\frac{\gamma\overline{w}}{H_m}$ is completely determined by the basic state. When SST increases, the vertical temperature gradient increases, and entrainment provides a greater heat flux into the mixed layer to oppose the SST change. The damping increases as the entrainment rate increases or as the mixed layer shoals.

The pure growth effect associated with the equatorial thermocline slope, h'_p, arises because adjustment of the slope is accomplished mainly by equatorial Kelvin waves, which require only a month or two to reach the eastern boundary. At interannual timescales, the anomalous slope is nearly in phase with the zonal wind stress anomaly and therefore with SSTA. When surface warms in the east, the trades weaken and the thermocline rapidly deepens in the east. This warms the subsurface, decreases the entrainment cooling of the mixed layer, and thereby reinforces the initial SST change.

The transitioning effect associated with the zonal-mean thermocline depth h'_m is more

subtle, as there are several processes which affect the heat content of the equatorial band. First, the *generation* of equatorial waves, in response to wind stress changes, produces meridional divergence in the basin interior. A westerly stress perturbation initially gives rise to equatorial downwelling, vortex squashing, convergence onto the equator, and a downwelling Kelvin signal; off-equator, meridional divergence shoals the thermocline and produces a pair of upwelling Rossby signals. Wave *reflections* are also essential, as when wave signals reach the boundaries, they generate narrow boundary currents which pump mass off-equator. Rossby waves reflected from the eastern boundary are eroded by dissipation as they propagate westward, and so are unable to propagate the thermocline depression far into the interior; the thermocline slope they produce is too strong to balance the westerly stress and so poleward currents develop which further discharge mass from the equatorial band. If the boundaries are gappy or slanted, or downward wave propagation is taken into account, then the reflections will be *imperfect* and some mass will effectively leak through the boundaries; at the equator, mass leaks in through the western boundary and out through the eastern boundary during a westerly event.

At interannual timescales, sharp Kelvin and Rossby wavefronts are absent and one may consider the ocean to be nearly adjusted. For equatorial westerlies, this means that equatorial heat content is being discharged by interior meridional divergence and outflux through the eastern boundary, and recharged by influx through the western boundary. The net effect at the equator is generally a small residual and is therefore sensitive to the magnitude of the stress curl and the reflectivity of the boundaries. For westerly stress anomalies, h'_m is discharged at the equator when (1) the wind stress anomaly is narrow in the meridional so that it produces strong interior divergence from the equatorial band, and (2) the boundaries are reflective enough in the west and leaky enough in the east that there is little net influx through the boundaries in the equatorial band.

These conditions are met in the intermediate model control run, and so there is a delayed negative feedback on the eastern Pacific thermocline depth, illustrated schematically by the $\widetilde{h}'_m$ phasor in Fig. 6.4. Interestingly, the phase delay is greater than 90° so the "negative feedback" is actually a destabilizing term. This component is also a *transitioner* which carries the system between events. The off-equator responds only slowly to changes in wind stress, so the discharge of equatorial heat content remains strong even after a warm event has ended and westerlies have decayed away. This plunges the system into a cold event and the cycle repeats with opposite sign. Thus the net effect of subsurface temperature changes on SST, $-\overline{w}\frac{\widetilde{\partial_z T'}}{\widetilde{T'}}$, results from a delicate balance of strong and competing effects.

Similar arguments hold for $-\frac{\widetilde{u}'}{\widetilde{T}'}\partial_x \overline{T}$, since the thermocline depth and zonal current are dynamically linked through geostrophy (An and Jin, 2001). Differentiating (4.2), in the inviscid limit without meridional convergence of the meridional wind stress, gives

$$U_1(y=0) = -\frac{c^2}{\beta}\,\partial_{yy} h_1|_{y=0} \tag{6.7}$$

so that the depth-averaged component of the equatorial zonal current is related to the meridional curvature of the thermocline. When the equatorial thermocline is depressed relative to the off-equator, there will be eastward geostrophic currents at the equator. Thus the slow discharge of heat content out of the equatorial band during warm events

is associated with the development of westward equatorial current anomalies, which act in concert with the equatorial shoaling to reverse the SSTA tendency and transition the system into a cold event. The smaller Ekman component of the equatorial zonal current is in phase with the zonal stress, since from (4.13)

$$U_s(y=0) = \frac{\tau_x(y=0)}{\rho r_s} \tag{6.8}$$

Thus the zonal advection term $-\frac{\widetilde{u}'}{\widetilde{T}'}\partial_x\overline{T}$ plays both transitioning and destabilizing roles in the control run.

6.2.4 Effects of changes in the background state

Figs. 6.3 and 6.4 summarize the linear dynamics of the control run in a concise way. Since these diagrams explicitly represent the role of the mean state, they may be useful in understanding and predicting the ENSO response to climate changes.

A change the background state has two effects. First, it selects *which* processes dominate the SST tendency; this is represented by the *magnitude* of the vectors in the phasor diagram. Second, it alters *how* those processes affect the growth rate and period; this is represented by the *phase* of the vectors in the phasor diagram. The latter is the more complicated effect, since the phasing of some terms may depend on the detailed spatial structure of the mode.

Let us explore the effect of changing a single basic state parameter in each tendency term, with the amplitudes and phases of all other tendency terms held fixed. Taking Figs. 6.3 and 6.4 as an example, one could predict that increasing the climatological vertical temperature gradient $\partial_z\overline{T}$ would destabilize the ENSO mode but have no effect on its frequency. Increasing the mean upwelling $\overline{w}$, the mean zonal temperature gradient $\partial_x\overline{T}$, or the entrainment temperature sensitivity b to thermocline depth would destabilize the mode as well, but would also increase its frequency. Increasing the phase delay of the equatorial recharge (Fig. 6.4), as might happen if the anomalous stress response shifted east or if the wave speed c slowed from reduced active layer depth H, would tend to increase the growth rate and decrease the frequency of ENSO. If nonlinearities are weak, then the net impact of multiple changes in tendency terms will simply be the vector sum of the individual changes in the complex plane.

Thus an SST tendency phasor diagram can provide a clear picture of the mechanism and sensitivity of a climate model at any given point in space. We shall use such a diagram in Chapter 7 to help analyze and compare results from the intermediate model and GCM.

6.3 Sensitivity of the SST mode

In this section, we invoke the fast-wave limit and various other reasonable assumptions to permit a complete nonlocal description of the SST mode (Fig. 6.2; Neelin, 1991). The SST mode is common in coupled GCMs, especially when the oceanic resolution is so coarse that mean equatorial upwelling is weak (Cane, 1992; Neelin et al., 1992; Moore,

1995; Delecluse et al., 1998; Li and Hogan, 1999). It also appears to play a role in higher-resolution GCMs and the real world, where it determines the spatial structure and propagation of SST anomalies. There is evidence that related "mobile modes" were important in the 1993–94 warm event (Delcroix, 1998), and may also be relevant to the observed seasonal cycle (Chang, 1994; Chang and Philander, 1994; Xie, 1994).

6.3.1 Equatorial fast-wave limit

Focusing on the equator and assuming meridional symmetry, we begin with the linearized SSTA equation (6.1) in the absence of horizontal mixing:

$$\partial_t T' = -u'\partial_x \overline{T} - \overline{u}\partial_x T' - w'\partial_z \overline{T} - \overline{w}\partial_z T' - \epsilon T' \tag{6.9}$$

The anomalous vertical temperature gradient is linearized as

$$\partial_z T' = \frac{\gamma}{H_m}\left(T' - bh'\right) \tag{6.10}$$

Ignoring dissipation and focusing on low-frequency motions so that the fast-wave limit is valid, (4.1) and (4.7) become

$$\partial_x h' = \frac{\lambda_h \tau_x'}{\rho c^2} \tag{6.11}$$

In this limit the active-layer currents vanish ($u_{al} = 0$), and the surface currents are due entirely to the part of the Ekman circulation not balanced by pressure gradients. Combining (4.15)–(4.16) then gives

$$u' = \frac{B\tau_x'}{\rho r_s H_m} \tag{6.12}$$

where

$$B \equiv \frac{H - H_m}{H} \tag{6.13}$$

Anomalous equatorial upwelling is given by (C.8), which in the limit of small r_s reduces to

$$w' = -\frac{B\beta\tau_x'}{\rho r_s^2} \tag{6.14}$$

For simplicity, we assume the zonal stress anomaly is proportional to the SST anomaly with a zonal phase shift. As we will be looking at normal modes with a sinusoidal structure in the zonal direction, we can induce a zonal phase shift by multiplying the SSTA by a complex scalar A:

$$\tau_x' = AT' = |A|\, e^{i\theta_A} T' \tag{6.15}$$

so that the stress anomaly is shifted eastward relative to the SST anomaly by a phase angle of θ_A. Observations indicate $\theta_A \approx -60°$, i.e. a westward shift of the stress anomaly relative to SSTA.

6.3.2 SST mode dispersion relation

Applying the normal mode structure

$$\left(T', h', u', w', \tau_x'\right) = \left(\widetilde{T}', \widetilde{h}', \widetilde{u}', \widetilde{w}', \widetilde{\tau_x}'\right) e^{\omega t - ikx} \tag{6.16}$$

with k strictly positive, and substituting these solutions into (6.9)–(6.15) gives

$$\omega = -\frac{\widetilde{u}'}{\widetilde{T}'}\partial_x\overline{T} + ik\overline{u} - \frac{\widetilde{w}'}{\widetilde{T}'}\partial_z\overline{T} - \overline{w}\frac{\widetilde{\partial_z T'}}{\widetilde{T}'} - \epsilon \tag{6.17}$$

$$\frac{\widetilde{u}'}{\widetilde{T}'} = \frac{BA}{\rho r_s H_m} \tag{6.18}$$

$$\frac{\widetilde{w}'}{\widetilde{T}'} = -\frac{\beta BA}{\rho r_s^2} \tag{6.19}$$

$$\frac{\widetilde{\partial_z T'}}{\widetilde{T}'} = \frac{\gamma}{H_m}\left(1 - \frac{ib\lambda_h A}{k\rho c^2}\right) \tag{6.20}$$

where all parameters are positive, except for $\overline{u}$ and $\partial_x\overline{T}$ which are negative and A which is complex. Combining these equations gives the dispersion relation

$$\omega = \frac{BA}{\rho r_s}\left(\frac{\beta\partial_z\overline{T}}{r_s} - \frac{\partial_x\overline{T}}{H_m}\right) + \frac{ib\lambda_h A\gamma\overline{w}}{k\rho c^2 H_m} - \left(\frac{\gamma\overline{w}}{H_m} + \epsilon\right) + ik\overline{u} \tag{6.21}$$

where the terms have been grouped according to their phase. The first term, which is in phase with the wind stress anomaly, represents the anomalous currents acting on the mean temperature structure. The second term, which is shifted 90° east of the stress anomaly, represents the effect of subsurface temperature changes acting through mean upwelling. The third term represents a pure damping in phase with the SST anomaly. The final term simply Doppler-shifts the frequency as the wavetrain is advected by the mean zonal currents.

6.3.3 SST mode phase relationships

Dynamical parameters for the intermediate model are listed in Table 4.2, and for the control run at 140°W in the equatorial Pacific we have $H = 120$ m, $c = 2.4$ m/s, $B = 0.58$, $|A| = 0.2$ dPa/°C, $\theta_A = -60°$, $\partial_x\overline{T} = -7.7 \times 10^{-7}$ °C/m, $\partial_z\overline{T} = 0.013$°C/m, $b = 0.075$°C/m, $\overline{u} = -0.25$ m/s, $\overline{w} = 1.5 \times 10^{-5}$ m/s. Assuming a zonal wavelength of 100° longitude, roughly two-thirds the size of the basin, gives $k = 5.7 \times 10^{-7}$ m^{-1}. For these parameters the SST mode has a period of about 1 year, is strongly damped (3 month e-folding time), and propagates westward with a phase speed of about 30 cm/s. The dispersion relation for these parameters is illustrated schematically in Fig. 6.5. This diagram completely describes the SST mode, including its structure, period, growth rate, propagation, parameter sensitivity, and climate sensitivity.

Propagation is essential to the frequency of this mode. Standing modes of this type can only arise if the SSTA phase propagation exactly opposes $\overline{u}$ (i.e. a Doppler-shifted standing mode), or if external forcing and/or delayed oceanic adjustment are present. The

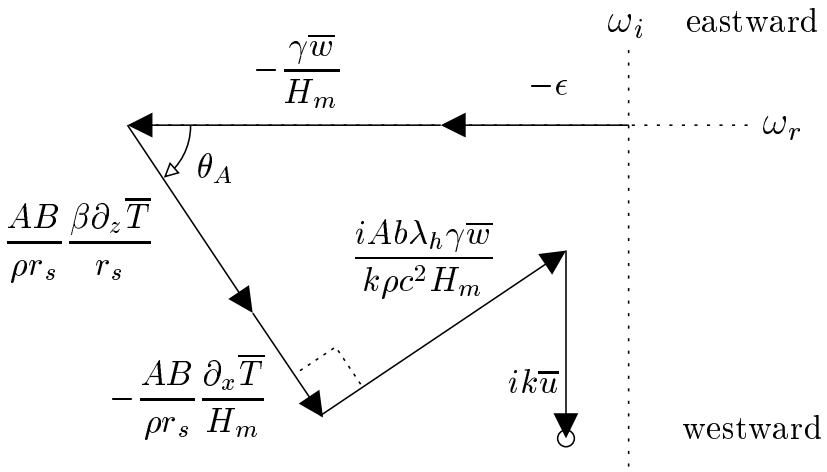

Figure 6.5: Schematic illustration of the complex frequency of SST anomalies for the SST mode (circle), which results from a combination of advective and surface flux tendencies (vectors). The mode has a sinusoidal structure in the zonal direction with positive wavenumber k. Real axis (ω_r) is the e-folding growth rate of the mode: positive is growing, negative is decaying. Imaginary axis (ω_i) is the angular frequency in time: positive is eastward-propagating, negative is westward-propagating. The counter-clockwise angle of each vector from the positive real axis indicates its eastward phase shift relative to SSTA. Vector directions and magnitudes approximate those seen in the intermediate model, for reasonable values of the parameters.

phase propagation arises from a competition of local and nonlocal processes. A westerly stress anomaly, for example, induces a warming *local* to the stress by reducing equatorial upwelling and advecting the warm pool eastward. However, it also induces a *nonlocal* warming by deepening the thermocline a quarter-cycle east of the stress anomaly, which warms that location via mean upwelling. The phase θ_A of the stress anomaly relative to SSTA is therefore key in determining the direction of propagation, as can be seen in Fig. 6.5. As θ_A increases from $-90°$ to $0°$ and the stress becomes more aligned with SST, the "current feedback" goes from inducing westward propagation to inducing growth, while the "thermocline feedback" goes from inducing growth to inducing eastward propagation. Thus the dynamics and sensitivity of the SST mode depend fundamentally on the zonal phase of the stress response to SSTA.

The strength of the thermocline feedback is proportional to the zonal wavelength, since as the wavelength increases the ocean integrates over a larger fetch of the stress anomalies and this results in a larger perturbation in the thermocline. For the observed phasing near $\theta_A = -60°$, it is clear that modes with long zonal wavelengths (small k) are more unstable (and propagate westward more slowly) than modes with short wavelengths. Thus variability will tend to favor the basin scale, where (for the parameters listed above) the SST mode is unstable and nearly stationary. At this scale one would expect boundary reflections to enter into the dynamics of the SST mode. For this reason, variability in coupled models and observations is often described in terms of "mixed modes" which involve elements of both the SST mode and basin wave dynamics modes. In these terms the SST mode can be viewed as controlling the growth and spatial structure of the variability, while ocean dynamics (including equatorial recharge/discharge) control the transitions and thereby set the time scale of the variability.

6.3.4 Effects of background changes on the SST mode

The climate sensitivity of the SST mode is clear from Fig. 6.5. Strengthening the mean temperature gradients $\partial_x \overline{T}$ and $\partial_z \overline{T}$ would destabilize this mode and increase its westward phase speed. Strengthening the mean zonal currents $\overline{u}$ would not affect the stability of the mode, but would increase the westward phase speed by advecting the mode westward. Increasing the mean upwelling $\overline{w}$ would strengthen the thermocline feedback and reduce the westward phase speed; the effect of $\overline{w}$ on the mode stability would depend on the strength of the subsurface temperature anomalies, as the increased upwelling would also act to damp SST anomalies. Increasing the sensitivity b of the entrainment temperature to thermocline depth anomalies (as might occur with a change in the climatological thermocline depth) would strengthen the thermocline feedback, destabilizing the SST mode and slowing its westward propagation. Finally, an increase in the active layer depth H would increase c and B, which in the absence of other changes would favor the current feedback over the thermocline feedback, leading to greater westward propagation, although the effect on stability would be parameter-dependent.

6.4 Summary

This chapter has provided a theoretical basis for understanding the effect of the tropical Pacific climatology on ENSO. A review of previous studies indicated that two coupled modes, the delayed/recharge oscillator and the SST mode, are useful prototypes for understanding ENSO behavior in a wide variety of models. Changes in climate parameters, such as the depth of the thermocline in the eastern Pacific, the intensity of the zonal SST contrast, and the strength of equatorial upwelling, affect the properties of these modes and the merger between them. A local linear analysis of the SST tendency equation in the intermediate model motivated a phasor diagram which illustrates key mechanisms and indicates climate sensitivities. Analysis of the SST mode in the fast-wave limit provided further insight into the structure and propagation of equatorial SST anomalies. The theoretical insights and phasor diagrams developed here are applied in the next chapter, which explores the simulated ENSO sensitivity to climate changes in the intermediate model and the hybrid coupled GCM.